Interactive Approach to Surface Fitting Complex Geometries for Flowfield Applications

F. McNeil Cheatwood* and Fred R. DeJarnette†
North Carolina State University, Raleigh, North Carolina
and
H. Harris Hamilton II‡
NASA Langley Research Center, Hampton, Virginia

Numerical flowfield methods require a geometry subprogram that can calculate body coordinates, slopes, and radii of curvature for typical aircraft and spacecraft configurations. The objective of this paper is to develop a new surface fitting technique that addresses two major problems with existing geometry packages: computer storage requirements and the time required of the user for the initial setup of the geometry model. In the present method, coordinates of cross sections are fit in a least-squares sense using segments of general conic sections. After fitting each cross section, the next step is to blend the cross-sectional curve fits in the longitudinal direction using general conics to fit specific meridional half-planes. For the initial setup of the geometry model, an interactive, completely menu-driven computer code has been developed to allow the user to make modifications to the initial fit for a given cross section or meridional cut. Graphic displays are provided to assist the user in the visualization of the effect of each modification. The completed model may be viewed from any angle by using the code's three-dimensional graphics package. Geometry results for the modeling of the Space Shuttle and a proposed aeroassist flight experiment (AFE) geometry are presented. Numerical results show that the accuracy of the geometry model can have a significant effect on the flowfield calculations.

Nomenclature

A_i = coefficients of global general conic equation (1), $i = 1,...,6$
A,B,C,D,E = coefficients of local general conic equation (2)
B_k,C,D_k = coefficients of nose fit, Eq. (6)
$\tilde{c}$ = length of wing chord at the given spanwise location; used to define spanwise cuts
r,ϕ = polar coordinates measured from the global origin ($X = 0, Y = 0$) in a given cross section; used to define meridional cuts
R = radius of curvature of the body at the nose
$\bar{R}$ = radius of circular arc for the AFE skirt
x,y = local Cartesian coordinate system
$\tilde{y}$ = chordwise distance from the wing leading edge at a given spanwise station; used to define spanwise cut locations
X,Y,Z = global Cartesian coordinate system
δ = rake angle of AFE geometry
ε_b = ellipsoid ellipticity in the YZ plane; parameter of AFE geometry
θ = orientation of local coordinate system with respect to global coordinate system
θ_{YZ} = elliptical cone half-angle in the symmetry plane of the AFE geometry
τ = angular extent of the circular-arc skirt in the upper symmetry plane of the AFE geometry
Ω = angle used in Eq. (15) to define the constant percent chord spacing

Subscripts

ASTUD = advanced surface-fitting technique featuring user-friendly development; results using current method
k = curve identification ($k = U$ for upper surface; $k = L$ for lower surface)
L = lower surface of nose region
QUICK = results using model created from the QUICK geometry package
ref = value based on the meridional cut nearest the requested value for ϕ; used during the interpolation process
U = upper surface of nose region
XZ = XZ plane
YZ = YZ plane
Z = partial derivative with respect to Z
ϕ = partial derivative with respect to ϕ

Superscripts

$( )'$ = first derivative with respect to the argument
$( )''$ = second derivative with respect to the argument

Introduction

NUMERICAL flowfield methods require a geometry subprogram that can calculate body coordinates, slopes, and radii of curvature. The coordinates and slopes are required for such techniques as the HALIS inviscid flowfield code,[1] whose pressure distribution solution may be used to drive a boundary-layer code. In addition, the radii of curvature must be supplied for methods that calculate inviscid surface streamlines from the pressure distribution.[2] In this paper, a new surface fitting technique is developed that addresses two major problems with existing geometry packages: computer storage requirements and the time required of the user for the initial setup of the geometry model.

Presented as Paper 87-1476 at the AIAA 22nd Thermophysics Conference, Honolulu, HI, June 8–10, 1987; received Oct. 6, 1987; revision received March 16th, 1988.

*Graduate Student, Aerospace Engineering. Student Member AIAA.
†Professor, Mechanical and Aerospace Engineering Department. Associate Fellow AIAA.
‡Research Leader, Aerothermodynamics Branch, Space Systems Division. Member AIAA.

Previous approaches to the surface fitting of three-dimensional bodies generally divided the surface into panels. If the panels are represented by flat surfaces,[3,4] then the body slopes are discontinuous at the edge of the panels. Coons' method,[5] which provides for continuous slopes and curvature, involves the specification of 64 parameters for each panel (or patch), many of which are difficult to obtain (most notably the cross derivatives).[6] In addition, computer storage requirements may be great when a large number of patches are required to describe a geometry. Using spline functions[7] to generate the surface fit often yields undesirable wiggles, dimples, or bulges in the resulting model. The QUICK method[8] is reasonably accurate, but the development of a given model requires a large initial setup time. Later supplements to this code allow the user to interactively and iteratively specify the cross-sectional and longitudinal curve fits that define the surface fit.[9]

DeJarnette and Ford[10] used general conic equations for the cross-sectional curve fits and blended them longitudinally by using parametric splines. Unfortunately, the use of parametric splines to describe the longitudinal variation of cross sections can yield the same undesirable qualities that plagued the usage of general splines in that capacity. The approach developed in Ref. 10 for curve fitting the cross sections is also used in Refs. 11 and 12, although the method for longitudinally blending these cross-sectional fits is altered. In Sliski's approach,[11] the longitudinal variation of cross sections is defined by one of several equations (including general conics and quadratic splines). Sliski's algorithm provides an accurate method for calculating body coordinates and surface derivatives, but it can be difficult to implement. Reference 12 discusses a method similar to the current research endeavor in that the longitudinal fit is handled by taking the same approach used to curve fit the cross sections and applying it to specified meridional cuts. However, the package is cumbersome to use when modeling complex geometries that have drastic changes in longitudinal body curvature. Reference 13 discusses an ongoing investigation into the use of Bezier curves to surface fit geometries.

It is advantageous to use conic sections rather than cubic or higher-order polynomial equations because they eliminate the possibility of unspecified inflection points in the fit. Therefore, the present technique also uses the cross-section curve fitting technique developed in Ref. 10. As with the approach described in Ref. 12, these cross-sectional curve fits are then blended in the longitudinal direction, again using conic equations applied to specific meridional cuts.

Since the surface fitting process for an arbitrary geometry is not a straightforward process, provisions should be made to allow the user to modify the current fit with minimal difficulty. Carrying out this procedure interactively eliminates the need for the user to construct lengthy input files, which can increase the initial setup time for the model. The creation of such files requires a greater understanding of the code by the user than an interactive, menu-driven code, which allows even a novice to use the code successfully. Graphics routines supplementing these menus help the user to visualize the effects of the specified changes on the surface fit.

Fitting the Fuselage Cross Sections

To construct a geometry model, a set of data points composed of cross-sectional coordinates at various axial locations along the fuselage is necessary. The first step in the surface fitting process involves curve fitting each of these fuselage cross sections of coordinates. In many cases, a smooth fit that passes through every data point in a given cross section cannot be realized. In Ref. 10, a technique that involves dividing a given cross section into *arcs* is developed (Fig. 1). Each arc is then curve fit to the coordinates in a least-squares sense with a general two-dimensional conic equation. This technique is the basis for the present method; its approach is outlined subsequently.

A portion of a general conic is curve fit in a least-squares sense through the data points of a given arc. The data points at each end of this arc are referred to as *control points*. The curve for this arc is constrained to pass through these two control points. The slope at each of these control points is constrained to be continuous with each of the two adjacent arcs, unless the slope at a control point has been specified by the user. If no slope specification is made at a given control point, then the value for the slope there is left as part of the solution. A slope specification may be in the form of a discontinuity or continuous slope. In either case, the user must specify the values for the slopes. Alternately, a given arc may be defined to be a *line segment* (see Fig. 1). The control point locations and slope specifications are defined interactively by the user with the aid of the graphics features of the program. These features are documented in Ref. 14.

That portion of a cross section between a beginning slope specification and an end slope specification is referred to as a *fitting region*. Such a fitting region may contain one or more arcs. The latter case occurs when no slope specifications are made at the control points between adjacent arcs (see Fig. 1). In such a case, the conic equations for each arc are determined simultaneously in order to provide continuous slopes at these intermediate control points. On the other hand, there is no constraint to make the second derivative continuous at the control points. A fitting region may encompass the entire cross section (if only the first and last control points have slopes specified) or as few as three data points (three points with two slopes give five constraints for the five coefficients of the general conic).

With the preceding overview in mind, define a Cartesian coordinate system whose origin is at the nose of the fuselage, with Z in the axial direction, X in the spanwise direction, and Y perpendicular to the XZ plane (Fig. 2). The present method assumes that the fuselage is symmetric about the YZ plane. For a given cross section of the fuselage, $Z = \text{const}$ and the global general conic equation for one arc is of the form

$$A_1X^2 + A_2XY + A_3Y^2 + A_4X + A_5Y + A_6 = 0 \qquad (1)$$

with its global coefficients A_1 through A_6.

In the curve fitting of a given arc, it is convenient to define a *local* coordinate (x,y) system whose origin is the first control

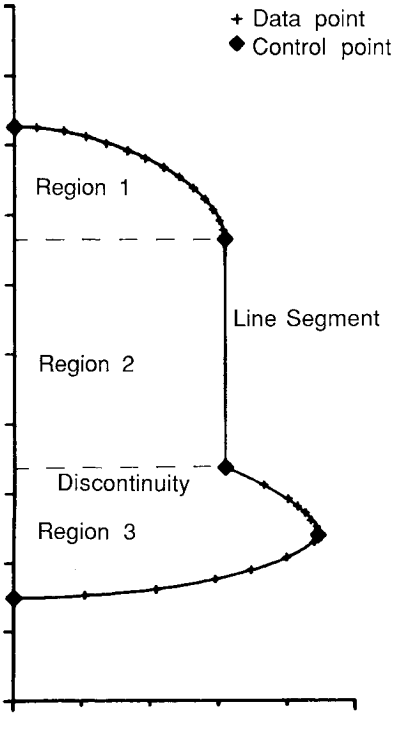

Fig. 1 Slope specifications and fitting regions in a cross section.

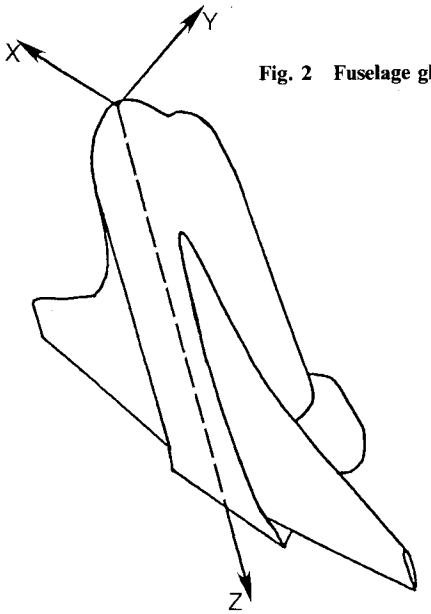

Fig. 2 Fuselage global coordinate system.

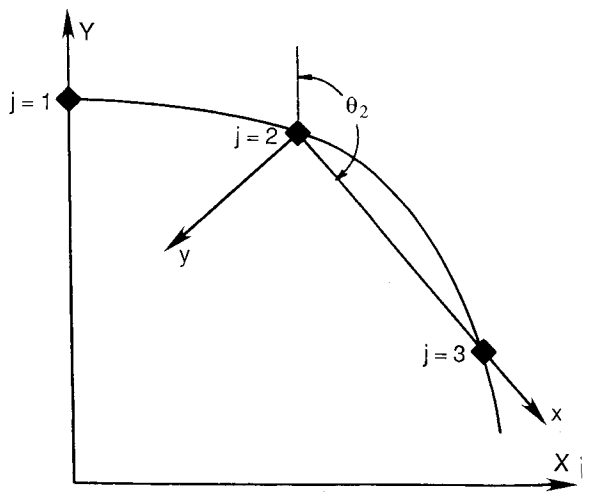

Fig. 3 Local coordinate system, illustrated for arc $j = 2$.

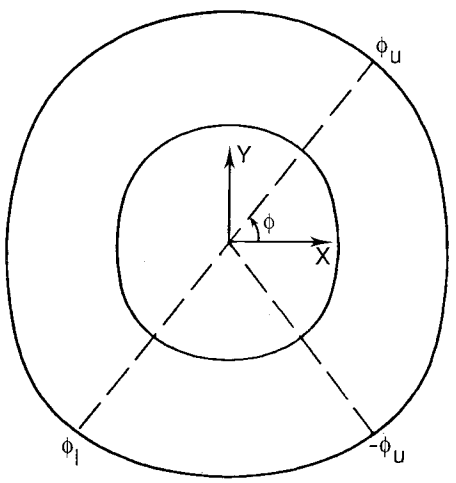

Fig. 4 Intersections between meridional cut and the two defining cross sections of the nose region.

point of the arc and whose x-axis passes through the second control point (Fig. 3). In this coordinate system, the local general conic equation is

$$Ax^2 + Bxy + Cy^2 + Dx + Ey = 0 \tag{2}$$

which inherently passes through the first control point ($x = 0$, $y = 0$). The procedure for evaluating A, B, C, D, and E (and determining which sign to use in the quadratic expression for x or y) is given in Ref. 10. Once the coefficients A, B, C, D, and E are known, they may be transformed into the global coefficients of Eq. (1) through a rotation of the local coordinate system.

Fitting the Nose Region

The *nose region* of the fuselage is treated separately from the remainder of the fuselage. The approach taken here allows for a unique specification of the nose region based on any two cross sections near the nose of the fuselage. For a given meridional ($\phi = \text{const}$) half-plane, the intersections between this half-plane and the conic fittings for the two cross sections are found (Fig. 4). These intersection points, along with the nose point ($r = 0$, $Z = 0$), are curve fit in the meridional half-plane (Fig. 5) using a conic equation constrained to pass through the nose point with an infinite value for the derivative r_Z. This equation is

$$r^2 + B_U Z^2 + CZ + D_U rZ = 0 \tag{3}$$

for the upper surface ($\phi = \phi_U$). The equation for the complement of this meridional half-plane ($\phi = \phi_L = \phi_U - \pi$) is

$$r^2 + B_L Z^2 + CZ + D_L rZ = 0 \tag{4}$$

which is on the lower surface. The coefficients for these two equations (henceforth referred to as a meridional *pair*) are evaluated simultaneously for a given value of ϕ_U. Because of symmetry, the curve fit for $\phi = \phi_L$ is identical to the curve fit for $\phi = -\phi_U$ (see Fig. 4). Thus, for a symmetric fuselage, a set of meridional pairs where $0 \le \phi \le \pi/2$ will encompass the entire fuselage since this gives $-\pi/2 \le \phi \le 0$. The coefficients (B_U, B_L, C, D_U and D_L) are constant for a given meridional pair but, in general, vary with respect to ϕ. It can be shown that the radius of curvature at the nose is given by

$$R(\phi) = -C(\phi)/2 \tag{5}$$

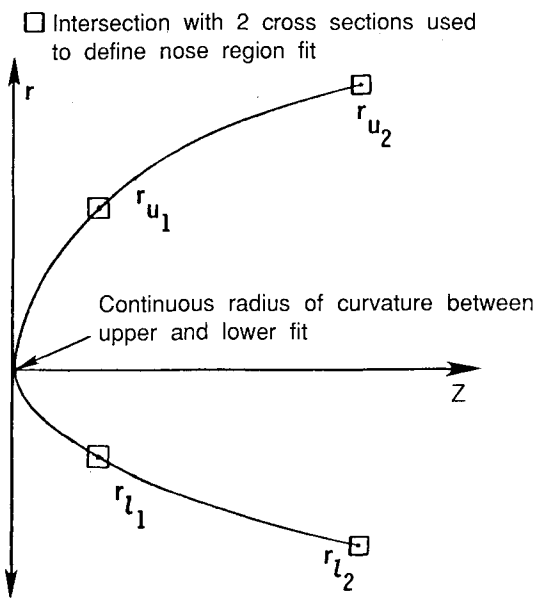

Fig. 5 Constraints on a given meridional cut in the nose region.

Since $C(\phi)$ is the same for the upper and lower equations, the radius of curvature is continuous between the upper and lower surfaces at the nose point.

Equations (3) and (4) can be written as the following single equation:

$$r^2 + B_k(\phi)Z^2 + C(\phi)Z + D_k(\phi)rZ = 0 \tag{6}$$

where $k = U$ for the upper surface and $k = L$ for the lower surface. The five coefficients (B_U, B_L, C, D_U, and D_L) must be evaluated for each meridional pair. The four intersection points between the meridional pair and the two cross sections give four constraints. For the fifth constraint, one option is to set

$$D_U(\phi) = -D_L(\phi) \tag{7}$$

Another option is to prescribe the nose radius of curvature in the XZ and YZ planes (R_{XZ} and R_{YZ}, respectively) and use an ellipsoidal variation in the circumferential direction. This gives

$$R(\phi) = [\sin^2\phi/R_{XZ} + \cos^2\phi/R_{YZ}]^{-1} \tag{8}$$

These five constraints provide five linear equations from which the coefficients B_U, B_L, C, D_U, and D_L can be calculated for any meridional angle ϕ. If Eq. (7) is used as the fifth constraint, the resulting radius of curvature distribution may be calculated from Eq. (5).

To determine slopes and second derivatives, differentiate Eq. (6) to obtain

$$r_\phi = -\frac{D'_k(\phi)rZ + B'_k(\phi)Z^2 + C'(\phi)Z}{2r + D_kz} \tag{9}$$

$$r_{\phi\phi} = -\frac{2[r_\phi + D'_k(\phi)Z]r_\phi + D''_k(\phi)rZ + B''_k(\phi)Z^2 + C''(\phi)Z}{2r + D_kZ} \tag{10}$$

$$r_Z = -\frac{(2B_kZ + C + D_kr)}{2r + D_kZ} \tag{11}$$

$$r_{ZZ} = -\frac{2\{(r_Z + D_k)r_Z + B_k\}}{2r + D_kZ} \tag{12}$$

$$r_{Z\phi} = -\frac{[2r_z + D_k]r_\phi + 2B'_kZ + C' + D'_k[r + Zr_Z]}{2r + D_kZ} \tag{13}$$

The equations for r_ϕ, $r_{\phi\phi}$, and $r_{Z\phi}$ involve first and second derivatives of the coefficients (B_U, B_L, C, D_U, and D_L) with respect to ϕ. These derivatives are obtained by applying Eqs. (9) and (10) at the four intersection points between the meridional pair and the two cross sections, combined with the ϕ derivatives of Eq. (7) or (8). The derivatives r_ϕ and $r_{\phi\phi}$ can be calculated from the cross-sectional curve fits in the two cross sections used for the nose region.

For the r_ϕ derivative, apply Eq. (9) at the four intersections, along with the first ϕ derivative of Eq. (7) or (8), to obtain five linear equations to evaluate B'_U, B'_L, C', D'_U, and D'_L. A similar procedure is used for the $r_{\phi\phi}$ derivative to evaluate B''_U, B''_L, C'', D''_U, and D''_L.

With the coefficients constrained in this fashion, the body radius (r) along with its first and second partial derivatives can be calculated for any (Z,ϕ) location within the nose region using Eqs. (6) and (9–13).

The program automatically calculates the coefficients for equations spanning (at discrete $\Delta\phi$ increments) the entire nose region ($-\pi/2 \le \phi \le \pi/2$). The user then may scrutinize this surface fit aided by the graphics routines. Should the fit prove to be unsatisfactory, the user may choose two other "constraining" cross sections or modify the nose radius of curvature distribution.

Longitudinally Blending the Fuselage Cross Sections

When all of the fuselage cross sections and the nose region have been fit satisfactorily, the next step is to *blend* the fuselage cross sections aft of the nose region in the longitudinal direction. This yields a set of equations that describe the entire fuselage surface.

The curve-fitting procedure used for the cross sections is also used for the longitudinal blending process, applied in $\phi =$ const (meridional) half-planes, because 1) smoothness of the "data points" (in this case, the intersections between each of the cross-sectional curve fits and the given meridional half-plane) is not guaranteed, 2) inflection points not controlled by the user are undesirable, and 3) surface discontinuities and line segments may be allowed. Thus, Eq. (1) is modified for use in the meridional half-plane:

$$A_1r^2 + A_2rZ + A_3Z^2 + A_4r + A_5Z + A_6 = 0 \tag{14}$$

The surface fit is handled by applying this equation to meridional cuts of the fuselage cross sections ($-\pi/2 \le \phi \le \pi/2$).

The approach of the current method differs from that of the method described in Ref. 12 in the following areas. In the latter, the longitudinal fitting process must be applied at every ϕ location where a body radius is to be evaluated. For a large number of surface points, this approach can lead to a significant amount of work for the user. In the current approach, the longitudinal fitting process is performed in the initial setup over the entire range of the fuselage ($-\pi/2 \le \phi \le \pi/2$) at discrete ϕ locations. The actual evaluations from the model are accomplished through a set of interpolation routines so that the body radius and its derivatives are known at any point on the surface of the geometry. In contrast, the method of Ref. 12 also requires that the first and second ϕ derivatives be longitudinally curve fit at every ϕ location where these derivatives are to be evaluated, thus requiring even more work of the user.

As with the cross sections, the meridional cuts are broken up into arcs through the specification of control points. The initial specifications place the first control point at the intersection between the meridional half-plane and the cross section specified to be the end of the nose region fit (recall that the nose fit is constrained to pass through this cross-sectional curve fit). The last control point is located at the intersection between the last cross section of the fuselage and the meridional half-plane. The longitudinal slope at the first control point is obtained from the nose region fit. Therefore, initially the longitudinal fit has a continuous slope across this juncture between the nose region fit and the fuselage afterbody.

In a manner analogous to the fuselage cross-sectional curve fitting procedure, the user curve fits a set of meridional cuts that encompass the entire fuselage beginning in the upper symmetry plane ($\phi = \pi/2$) and rotating around to the lower symmetry plane ($\phi = -\pi/2$). As with each of the fuselage cross-sectional curve fits, the curve fit for a given meridional cut is independent of the fits for the other meridional cuts. As a result, the longitudinal locations of the control points may differ from one meridional cut to another. In addition, the longitudinal slope specifications at these control points also may vary from meridional cut to meridional cut.

If these specifications do not yield a satisfactory fit for the current meridional cut, the user may modify them in the same manner as the cross sections were modified. When a range of meridional cuts encompassing the entire fuselage has been fit successfully, a plotting array is loaded automatically by the program. This allows the surface fit of the fuselage to be viewed by the user.

Surface Fitting the Wing

The technique used in curve fitting the fuselage cross sections is again employed here. It was decided that this approach could be most readily applied to the wing by defining a new coordinate system in which the coordinate corresponding to the axial direction of the fuselage would now correspond to the spanwise direction of the wing (Fig. 6). Furthermore, the wing cross sections (aligned perpendicular to the spanwise direction) assume the role previously played by the fuselage cross sections. As a result, sets of data points located at several discrete spanwise locations (analogous to the data point sets at discrete axial locations used for surface fitting the fuselage) are deemed necessary to achieve a good wing surface fit. Unlike the fuselage, no plane of symmetry is assumed for the wing. As with the longitudinal blending of the fuselage cross sections, the upper and lower surfaces of each wing airfoil section are curve fit separately.

In order to define the leading and trailing edges of the wing at any spanwise location, the planform of the wing must be curve fit. The coordinate system for this procedure is shown in Fig. 7. The "data points" used in this fitting are the leading- and trailing-edge chordwise locations (Y coordinates) for each wing cross section along with their corresponding spanwise positions (Z coordinates).

The process of blending the wing-sectional curve fits in the spanwise direction completes the definition of the wing surface. The concept of this procedure is similar to the one employed in the longitudinal blending of the fuselage cross sections. Here, however, constant percent chord cuts were found to be better than meridional cuts for the spanwise blending process.

In order to cluster points near the leading and trailing edges, the following transformation from airfoil theory is used:

$$\tilde{y}/\tilde{c} = (1 + \cos \Omega)/2 \qquad (15)$$

where $\tilde{y}$ is the chordwise distance from the wing leading edge, $\tilde{c}$ the chord of the wing at this spanwise location, and $0 \leq \Omega \leq \pi$ for the upper surface and $\pi \leq \Omega \leq 2\pi$ for the lower surface.

Applying Eq. (15) at the leading edge ($\tilde{y}/\tilde{c} = 0$), $\Omega = \pi$. At the trailing edge ($\tilde{y}/\tilde{c} = 1$), $\Omega = 0$ for the upper surface and $\Omega = 2\pi$ for the lower surface. By using Eq. (15) to define the locations of the blending cuts, these cuts are clustered near the leading and trailing edges of the wing.

The spanwise blending process of the wing sections begins at the trailing edge ($\Omega = 0$) and progresses toward the leading edge along the upper surface (at $\Delta\Omega = \text{const}$ intervals). Once the leading edge is reached, the spanwise blending process continues toward the lower surface moving from the leading edge back to the trailing edge using the same value for $\Delta\Omega$ that was used for the upper surface. As a result, both the upper and lower surfaces of the wing at a given $\tilde{y}/\tilde{c}$ location will be curve fit.

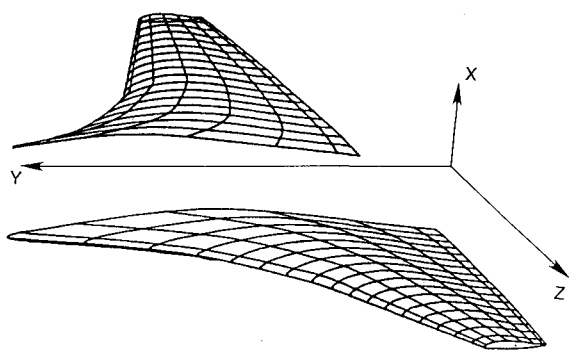

Fig. 6 Wing global coordinate system.

Interpolation Procedure

Thus far, the model consists of a set of equations that defines a number of longitudinal (fuselage) and spanwise (wing) curves at discrete ϕ and $\tilde{y}/\tilde{c}$ locations, respectively. This provides a skeleton of the model, where the cross-sectional curve fits serve as the bulkheads or ribs and the meridional curve fits are the stringers. To apply this model at locations between these defined curves, a set of interpolation routines was developed. For input values of the longitudinal (Z) and circumferential (ϕ) coordinates of the fuselage, this involves calculating the surface radius and derivatives based on the meridional curve fits in the *neighborhood* of ϕ.

Initially, a neighborhood of five meridional cuts at the prescribed value of Z was curve fit in the ϕ direction with a general conic equation. This curve passes through each of these five points. However, since the meridional cuts were curve fit independently of each other, a smooth variance in the ϕ direction is not guaranteed. As a result, this approach generally yielded a hyperbolic equation with imaginary roots (which is undesirable). Increasing this neighborhood to six cuts (and thereby curve fitting the points in a least-squares sense with the general conic) improved this situation, but some hyperbolic results still persisted. To resolve this problem, each neighborhood was curve fit in a least-squares sense with an X parabola, a Y parabola, and a line segment, in addition to the general conic. The equation that adhered most closely to the original meridional curve fits in the neighborhood of ϕ was then used to evaluate the surface radius and derivatives at that (Z,ϕ) location. A more thorough description of this procedure will be given.

First, the input value of Z is compared with the axial locations of the original fuselage cross sections of data. If this axial location lies within the nose region (Fig. 8), then the body radius and its derivatives are determined according to the nose

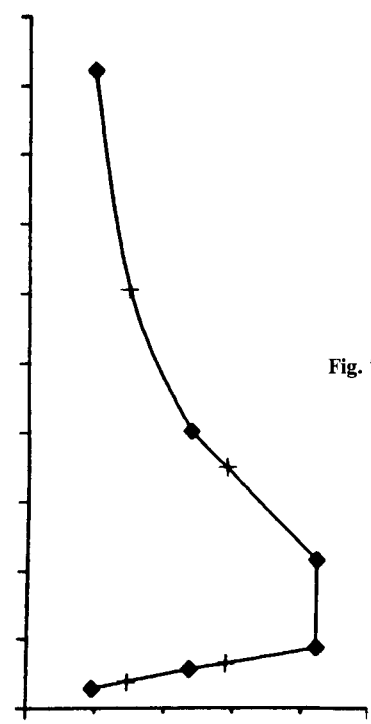

Fig. 7 Curve fit of wing planform.

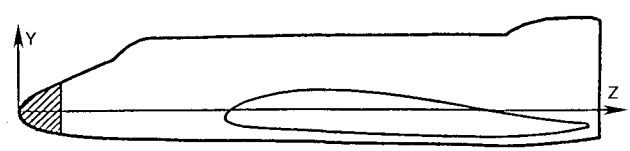

Fig. 8 Side view of fuselage surface fit with nose region highlighted.

region fit. However, if this axial location is beyond the nose region, then the following interpolation procedure must be exercised.

The input value of ϕ is compared with the locations of the meridional cuts that were curve fit during the initial model setup. The location of the meridional cut closest to but greater than ϕ (Fig. 9) is called ϕ_{ref}. The value of r at this (Z,ϕ_{ref}) location is called r_{ref}. Then the values for the body radii at Z using the curve fit equations for the six meridional cuts in the neighborhood of ϕ_{ref} are found (see Fig. 9). These points are curve fit in a least-squares sense with four conic equations: general conic, X parabola, Y parabola, and line segment.

After their coefficients have been evaluated, each of these equations is applied at ϕ_{ref}. Since the equations are curve fit in a least-squares sense, none of them is constrained to go through any of the meridional cuts. These resulting values for r are compared with r_{ref}, and the curve that yields the closest agreement with r_{ref} is used to evaluate r for the input value of ϕ. Thus, the equation that adheres most closely to the skeleton is used for the evaluation of r. These same coefficients also are used to evaluate r_ϕ and $r_{\phi\phi}$.

In a procedure analogous to the evaluation of r, the approach for determining r_Z is as follows. The values for r_Z at Z using the meridional cuts in the neighborhood of ϕ are calculated. These points are then fit in a least-squares sense with the same four types of conic equations as used previously. Each of these equations is applied at ϕ_{ref}. The curve that yields the closest agreement with $r_{Z,ref}$ is used to evaluate r_Z. Finally, the approach for determining r_{ZZ} is analogous to the procedure for determining r_Z.

Note that any discontinuities or line segments specified in the cross-sectional or longitudinal curve fits are preserved in this interpolation process. It should also be noted that, during the development of this approach, the equation selections were monitored, and it was found that the type of equation that yielded the best fit over the range of (Z,ϕ) locations varied. Therefore, it was determined that a selection process between the four types of conic equations was necessary to ensure the best possible surface fit. The approach for interpolating wing values is similar to the one used for the fuselage.

Results and Discussion

The accuracy of a model for a given geometry can have a significant effect on the results obtained from flowfield calculations. As an example, consider two models of the Space Shuttle. The first is simply a hyperboloid, which is axisymmetric by definition. This shape matches the windward plane of symmetry of the Shuttle geometry well, but the cross sections, wing, and canopy are not modeled. The second representation is the HALIS QUICK model.[1] This model was used in the HALIS inviscid flowfield code and it provides a good model of the windward surface of the Shuttle, including the wing.

Some results from a viscous/shock-layer code[15] using these two models are shown in Fig. 10. This heat-transfer comparison is for the windward symmetry plane of the Shuttle. It can be seen that the results using the QUICK model are in better agreement with the flight data than those obtained using the hyperboloid model. This improvement can be attributed to the fact that the QUICK model allows the flowfield calculations to take into account the effect of spanwise flow along the wing. In addition, the QUICK model properly accounts for the expansion region at the rear of the fuselage, whereas the hyperboloid does not. The geometry model generated using the current method gives results very close to those of the QUICK model for the windward plane of symmetry.

A geometry model for the Shuttle was created using the current method from a set of data points grouped according to fuselage cross sections. The complexities of this geometry provided an excellent test for the many features of this code. As the cross-section curve fitting process advanced along the fuselage away from the nose, the cross sections became increasingly more challenging, bringing with them the necessity to make the program more powerful.

For this Space Shuttle model, the nose radius of curvature was left as part of the solution, and the nose fit was constrained

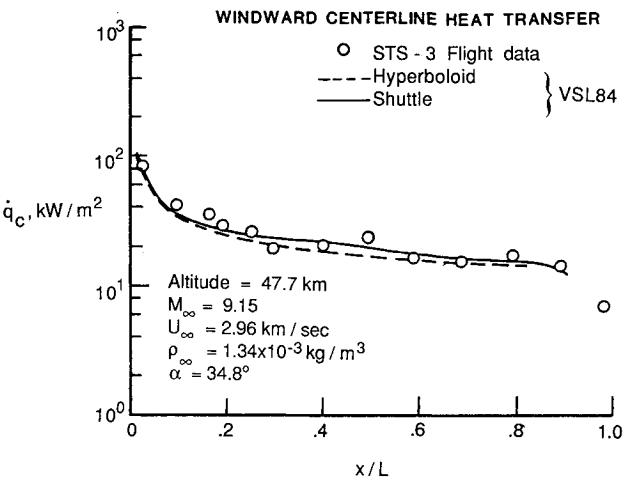

Fig. 10 Effect of accuracy of geometry model on viscous flowfield calculations.

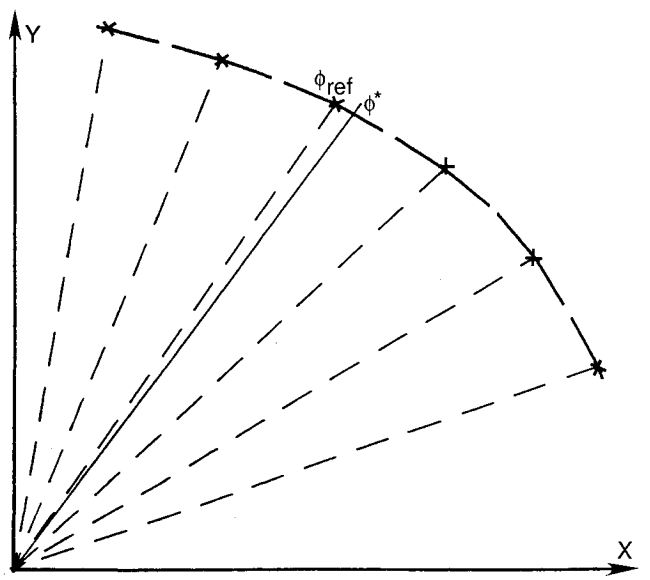

Fig. 9 Meridional cut neighborhood of ϕ^*.

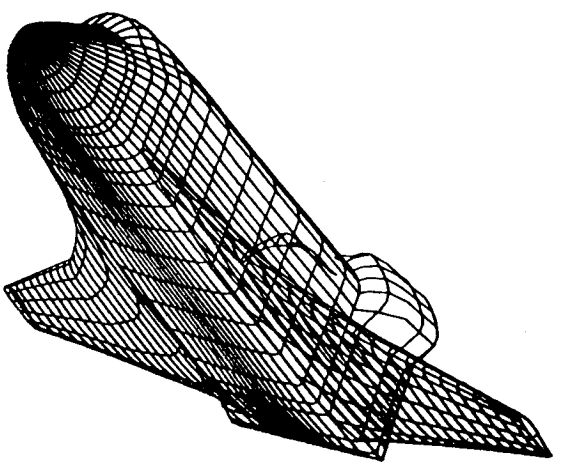

Fig. 11 Space Shuttle model created using current method.

Table 1 Sample cross section of AFE geometry comparison

	$Z = 0.68979E-1$					
ϕ,[a] deg	r	r_Z	r_ϕ	r_{ZZ}	$r_{Z\phi}$	$r_{\phi\phi}$
90.0	0.23765	1.2423	$0.41540E-8$	−40.562	$0.65588E-7$	$0.95033E-1$
	0.23766	1.2423	0.0000	−40.562	0.0000	$0.84623E-1$
67.5	0.24488	1.3729	$-0.36117E-1$	−48.999	−0.75219	$0.83610E-1$
	0.24418	1.3357	$-0.32760E-1$	−38.869	−0.51184	$0.76937E-1$
45.0	0.26362	1.9023	$-0.54363E-1$	0.0000	−0.39228	$0.33632E-1$
	0.25852	1.3173	$-0.60151E-1$	0.0000	−1.1398	$0.48285E-1$
22.5	0.28523	2.0583	$-0.48692E-1$	0.0000	−0.35137	$-0.72447E-1$
	0.28387	1.9014	$-0.61068E-1$	0.0000	−1.7366	$-0.84682E-1$
0.0	0.29588	2.1351	0.0000	0.0000	0.0000	−0.15374
	0.29582	2.1348	$0.36836E-2$	0.0000	$-0.83418E-1$	−0.20199
−22.5	0.28523	2.0583	$0.48692E-1$	0.0000	0.35137	$-0.72447E-1$
	0.28523	2.0566	$0.49535E-1$	0.0000	0.33478	$-0.77776E-1$
−45.0	0.26362	1.9023	$0.54363E-1$	0.0000	0.39228	$0.33632E-1$
	0.26359	1.8997	$0.55577E-1$	0.0000	0.39493	$0.44674E-1$
−67.5	0.24627	1.7771	$0.31341E-1$	0.0000	0.22616	$0.74647E-1$
	0.24628	1.7772	$0.31271E-1$	0.0000	0.23270	$0.64727E-1$
−90.0	0.24003	1.7321	$-0.35874E-8$	0.0000	$-0.25887E-7$	$0.82071E-1$
	0.24003	1.7321	0.0000	0.0000	0.0000	0.82039

[a]For a given value of ϕ, the first line shows the analytic results, and the second line shows the ASTUD results.

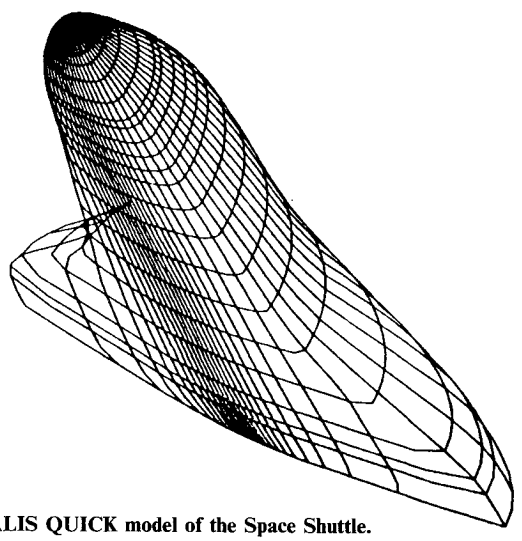

Fig. 12 HALIS QUICK model of the Space Shuttle.

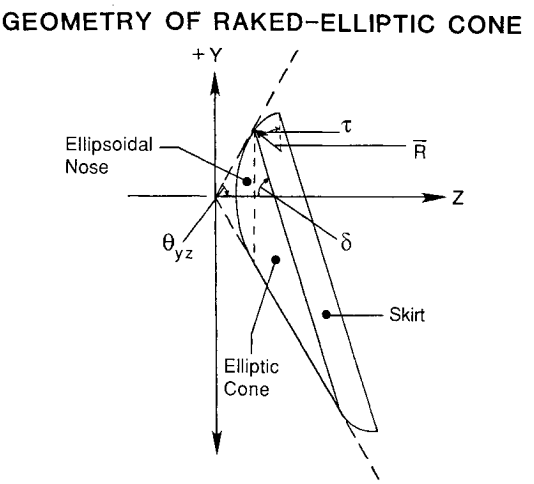

Fig. 13 Defining parameters of a proposed AFE geometry.

to pass through the curve fits of the second and third cross sections of the input coordinates. Wing cross-section data were also available, therefore, the wing-body combination was modeled (Fig. 11). (The actual calculation of the curve defining the wing-body intersection remains as an area of future work.) Using the interpolation routines, the agreement between this model, the original input data points, and the HALIS QUICK model were examined. Since the QUICK model used here does not attempt to model a large portion of the upper part of the fuselage (Fig. 12), comparisons between the two models and the original data are restricted, for the most part, to the windward surface of the fuselage and wing. It was found that both models are in good agreement with the original input coordinates for the majority of the compared portions of the geometry.

A geometry for the proposed aeroassist flight experiment (AFE)[16] was chosen as a second test case for the current geometry package. This configuration is a raked elliptic cone with an ellipsoidal nose and circular-arc skirt. An in-depth discussion of this geometry is given in Ref. 16, where, as shown, this body surface and its partial derivatives can be defined completely analytically. For this case, the following values were used in conjunction with the cylindrical afterbody option (Fig. 13):

$$\tau = \theta_{YZ} = 60 \text{ deg}, \quad \delta = 73 \text{ deg}, \quad \bar{R} = 0.1, \quad \text{and} \quad \varepsilon_b = 1$$

Next, 11 cross sections of 37 data points each (positioned at $\Delta\phi$ = 5-deg increments) were generated. The spacing for the cross sections and their data points was chosen arbitrarily, although the number of cross sections was intentionally kept small to tax the code's ability to model a geometry based on a minimal amount of input. This point is of interest because the number of cross sections used to generate the model dictates the time required for the user to surface fit a particular geometry.

Using these data planes, the AFE geometry was surface fit by a user (not an author of this paper) unfamiliar with the code and its operation. This modeling process was performed during several sessions, and the total time expended by the user (start-

ing from raw data, periodically modifying given curve fits, until the model was completed) was approximately 3 h. The results of this fitting procedure may be viewed as a "starting solution" for the geometry model; i.e., in scrutinizing a constructed model, the user may note areas where modifications are necessary before the model may be used satisfactorily in flowfield applications. Here, these "first-cut" results will be examined.

For this geometry, the nose region is constrained to pass through the first and second cross-sectional curve fits. Since the analytic equation for the nose region of this geometry is an ellipsoid, the nose radius of curvature may be determined easily. Based on the input parameters specified, it can be shown that

$$R_{XZ} = 0.6836643 \quad \text{and} \quad R_{YZ} = 0.4499019$$

It is found that the computed distribution of the nose radii of curvature based on these values of R_{XZ} and R_{YZ} is virtually identical to the distribution obtained when the nose radius of curvature is not specified by the user. This is to be expected, as shown in the following argument. The two cross sections chosen to model the nose region are indeed within the ellipsoidal nose region of the AFE geometry. Therefore, they are symmetric about the XZ plane. As a result, the coefficients for the upper and lower portions of a given meridional pair should be identical. Furthermore, since this ellipsoid is oriented along the Z axis, $D_U = D_L = 0$. Thus, when the nose radius of curvature is determined as part of the solution, not only is $D_L = -D_U \approx 0$ as assigned by the program, but the symmetry causes $B_L \approx B_U$. On the other hand, when the nose radius of curvature is specified, symmetry of the data causes $B_L \approx B_U$, $D_L \approx 0$, and $-D_U \approx 0$. Thus, the distributions of the nose radii of curvature shoud be nearly identical for the two nose region definitions.

In order to validate this AFE surface fit, the body radii and partial derivatives as calculated from the model are compared with their corresponding analytic values in Table 1. As a further test, the locations of these comparisons are chosen so as not to coincide with the cross sections and meridional cuts that were actually curve fit to generate the model. The results of this comparison, in general, show excellent agreement for the body radii, very good agreement for the first partial derivatives, and, for the most part, inconsistent agreement for the second partial derivatives (see Table 1).

In general, a model developed using this geometry package should meet the needs of a flowfield code that requires the geometry subroutine to calculate the surface coordinates and even first partial derivatives. However, the constructed model may not serve satisfactorily when the second partial derivatives also must be provided by the geometry subroutine.

Concluding Remarks

An interactive, user-friendly, completely menu-driven code for surface fitting arbitrary geometries has been developed. Provisions have been made to handle bodies, wings, and wing-body combinations. The present method calculates first and second partial derivatives, in addition to the body radius, for any point on the configuration. Geometry comparisons for the Space Shuttle and a proposed aeroassist flight experiment (AFE) geometry show good agreement between the values calculated from the models and those of the input coordinates (Space Shuttle) and actual geometry (AFE). Numerical results show that the accuracy of the geometry model can have a significant effect on the flowfield calculations.

Acknowledgment

Support for this investigation was provided by Cooperative Research Agreements NCC1-22 and NCC1-100 from NASA Langley Research Center.

References

[1]Weilmuenster, K. J. and Hamilton, H. H., II, "Calculations of Inviscid Flow Over Shuttle-Like Vehicles at High Angles of Attack and Comparisons with Experimental Data," NASA TP-2103, May 1983.

[2]DeJarnette, F. R. and Hamilton, H. H., II, "Inviscid Surface Streamlines and Heat Transfer on Shuttle-Type Configurations," *Journal of Spacecraft and Rockets*, Vol. 10, May 1973, pp. 314–321.

[3]Margason, R. J. and Lamar, J. E., "Vortex-Lattice Fortran Program for Estimating Subsonic Aerodynamic Characteristics of Complex Planforms," NASA TN D-6142, Feb. 1971.

[4]Woodward, F. A., "Analysis and Design of Wing-Body Combinations at Subsonic and Supersonic Speeds," *Journal of Aircraft*, Vol. 5, Nov.–Dec. 1968, pp. 528–534.

[5]Coons, S. A., "Surfaces for Computer-Aided Design of Space Forms," Massachusetts Institute of Technology, Cambridge, MA, Rept. MAC-TR-41, Contract AF-33(600)-42859, June 1967.

[6]Bezier, P., *Numerical Control Mathematics and Applications*, Wiley, New York, 1972.

[7]DeJarnette, F. R., "Calculation of Inviscid Surface Streamlines and Heat Transfer on Shuttle Type Configurations: Part I—Description of Basic Method," NASA CR-111921, Aug. 1971.

[8]Vachris, A. F. and Yeager, L., "QUICK-GEOMETRY, A Rapid Response Method for Mathematically Modeling Configuration Geometry," *Applications of Computer Graphics in Engineering*, NASA SP-390, Oct. 1975, pp. 49–73.

[9]Adams, M. S., "Interactive Input for the QUICK Geometry System—User's Manual," NASA TM-81933, Feb. 1981.

[10]DeJarnette, F. R. and Ford, C. P., "Surface Fitting Three-Dimensional Bodies," *Applications of Computer Graphics in Engineering*, NASA SP-390, Oct. 1975, pp. 447–474.

[11]Sliski, N. J., "A Numerical Technique for Describing Three-Dimensional Surfaces," Air Force Wright Aeronautical Lab., AFWAL-TR-3038, Sept. 1983.

[12]Perkins, J. N., "An Interactive Method for Surface Fitting Three-Dimensional Bodies," AIAA Paper 83-0220, Jan. 1983.

[13]Crisp, V. K., Rehder, J. J., and Schwing, J. L., "Intersection of Three-Dimensional Geometric Surfaces," NASA TP-2454, July 1985.

[14]Cheatwood, F. M., DeJarnette, F. R., and Hamilton, H. H., II, "An Interactive User-Friendly Approach to Surface-Fitting Three-Dimensional Geometries," NASA CR-4126, Mar. 1988.

[15]Thompson, R.A., "Three-Dimensional Viscous-Shock-Layer Applications for the Space Shuttle Orbiter," AIAA Paper 85-0246, Jan. 1985.

[16]Cheatwood, F. M., DeJarnette, F. R., and Hamilton, H. H., II, "Geometrical Description for a Proposed Aeroassist Flight Experiment Vehicle," NASA TM-87714, July 1986.